

NOTE

Accurate Numerical Solution of Charged Particle Motion in a Magnetic Field

1. INTRODUCTION

Recently, there appeared an analysis of the Boris algorithm [1] for large $\omega_c \delta t$ [2], where ω_c is the cyclotron frequency. This analysis and accompanying examples demonstrate that the Boris algorithm yields the correct rapid motion and drifts for small time steps ($\omega_c \delta t < 1$), and the correct drifts for large time steps ($\omega_c \delta t > 1$). This is an important result, especially for fully kinetic implicit plasma simulation on ion time scales, where the cost of constraining $\omega_{ce} \delta t < 1$ is prohibitively high (ω_{ce} is the electron cyclotron frequency). As the authors note, however, time-discretization errors cause the numerical gyroradius ρ_c and the physical gyroradius ρ_0 to be unequal for large δt . In fact, it can be shown that for $\omega_c \delta t > 1$, the numerical gyroradius increases linearly with δt in the Boris algorithm. Thus, an accurate value of the drifts is obtained only when the numerical gyroradius is smaller than the magnetic field gradient scale length ($\rho_c |\nabla B/B| < 1$, where B is the magnitude of the magnetic field \mathbf{B}). Then, the increasing numerical gyroradius that results from increasing δt in the Boris algorithm can compensate for numerical errors in the calculation of the drifts. However, when the numerical gyroradius exceeds the magnetic field gradient scale length ($\rho_c |\nabla B/B| > 1$), the particle no longer sees a uniform magnetic field as it samples the orbit, resulting in the wrong value for the drifts even when the drift equations are valid ($\rho_0 |\nabla B/B| < 1$).

Here, we compare the Boris algorithm with an alternative algorithm for the particle equations of motion that results in the correct drift motion whenever the drift equations are valid, even for very large values of the time step [3]. This algorithm combines an implicit Euler scheme with an additional term that gives the correct drifts and the correct size of the particle orbit (gyroradius) for all values of the time step. Since the alternative algorithm has already been shown by analysis and numerical tests to give the correct $\mathbf{E} \times \mathbf{B}$ drift and it can be shown trivially to give the correct polarization drift [3], the comparison with the Boris scheme is limited to magnetic-gradient-induced drifts.

2. NUMERICAL MODELS

For simplicity, we will consider the case in which the electric and magnetic fields are prescribed and time-independent. The particle equations of motion are given by

$$\begin{aligned} \frac{d\mathbf{u}}{dt} &= \frac{q}{m} (\mathbf{E} + \mathbf{u} \times \mathbf{B}) \\ \frac{d\mathbf{x}}{dt} &= \mathbf{u}. \end{aligned} \tag{1}$$

We will briefly describe the three numerical algorithms which are used to advance Eq. (1).

(A) *Method I* is a leapfrog Boris method in which the pair of variables \mathbf{x} and \mathbf{u} are advanced in time alternately. This is the algorithm used by Parker and Birdsall [2]. The equations of motion, Eq. (1), are advanced as follows:

$$\begin{aligned} \frac{\mathbf{u}_1 - \mathbf{u}_0}{\delta t} &= \frac{q}{m} \left(\mathbf{E}(\mathbf{x}_{1/2}) + \frac{\mathbf{u}_1 + \mathbf{u}_0}{2} \times \mathbf{B}(\mathbf{x}_{1/2}) \right) \\ \frac{\mathbf{x}_{1/2} - \mathbf{x}_{1/2}}{\delta t} &= \mathbf{u}_1. \end{aligned} \tag{2}$$

The subscript denotes the time level of the variable with, for example, $\mathbf{x}_{1/2} = \mathbf{x}((n + \frac{1}{2})\delta t)$, and $\mathbf{u}_1 = \mathbf{u}((n + 1)\delta t)$. With $\mathbf{E} = 0$, one can solve Eq. (2) for $(\mathbf{u}_1 + \mathbf{u}_0)/2$,

$$\frac{\mathbf{u}_1 + \mathbf{u}_0}{2} = \frac{\mathbf{u}_0 + \mathbf{u}_0 \times \left(\frac{q\delta t \mathbf{B}_{1/2}}{2m} \right) + \mathbf{u}_0 \cdot \left(\frac{q\delta t \mathbf{B}_{1/2}}{2m} \right) \left(\frac{q\delta t \mathbf{B}_{1/2}}{2m} \right)}{1 + \left(\frac{q\delta t \mathbf{B}_{1/2}}{2m} \right)^2}, \tag{3}$$

where $\mathbf{B}_{1/2} = \mathbf{B}(\mathbf{x}_{1/2})$. Given \mathbf{u}_0 and $\mathbf{x}_{1/2}$, one solves Eq. (3) for \mathbf{u}_1 , and the second part of Eq. (2) is used subsequently to calculate $\mathbf{x}_{3/2}$.

(B) *Method II* is an implicit method in which the pair of variables \mathbf{x} and \mathbf{u} are defined at the same time levels and are, therefore, advanced together [4], instead of being advanced alternately as in Method I. The equations of motion, Eq. (1), are advanced as

$$\frac{\mathbf{u}_1 - \mathbf{u}_0}{\delta t} = \frac{q}{m} \left(\mathbf{E}_{1/2} + \frac{\mathbf{u}_1 + \mathbf{u}_0}{2} \times \mathbf{B}_{1/2} \right) \tag{4}$$

$$\frac{\mathbf{x}_1 - \mathbf{x}_0}{\delta t} = \frac{\mathbf{u}_1 + \mathbf{u}_0}{2},$$

where

$$\mathbf{E}_{1/2} \equiv \mathbf{E} \left(\frac{\mathbf{x}_1 + \mathbf{x}_0}{2} \right)$$

$$\mathbf{B}_{1/2} \equiv \mathbf{B} \left(\frac{\mathbf{x}_1 + \mathbf{x}_0}{2} \right).$$

As before, the subscript denotes the time level of the variable. Note that with $\mathbf{E} = 0$, the solution to Eq. (4) is given by Eq. (3). Given \mathbf{x}_0 and \mathbf{u}_0 , Eq. (4) is used to calculate \mathbf{x}_1 and \mathbf{u}_1 . It is important to recognize that since the electric and magnetic fields must be evaluated at the mid-orbit position, one must iterate to solve Eq. (4).

(C) *Method III* is similar to Method II, except that an additional force, the $-\mu \nabla B$ force, is added explicitly to the usual Lorentz force to yield the correct value for the drifts when the time step is large [3]. The particle motion is advanced as

$$\begin{aligned} \frac{\mathbf{u}_1 - \mathbf{u}_0}{\delta t} &= \frac{q}{m} \left(\mathbf{E}_{1/2} + \frac{\mathbf{u}_1 + \mathbf{u}_0}{2} \times \mathbf{B}_{1/2} \right) - \mu \nabla B_{1/2} \\ \frac{\mathbf{x}_1 - \mathbf{x}_0}{\delta t} &= \frac{\mathbf{u}_1 + \mathbf{u}_0}{2}, \end{aligned} \tag{5}$$

where

$$\mu = \frac{[(\mathbf{u}_1 - \mathbf{u}_0) - (\mathbf{u}_1 - \mathbf{u}_0) \cdot \mathbf{B}_{1/2} \mathbf{B}_{1/2} / B_{1/2}^2]^2}{8B_{1/2}}. \tag{6}$$

One can show that the above expression for the magnetic moment μ can be recast in a different form from that given in [3], so that μ does not depend on the time-advanced velocity \mathbf{u}_1 explicitly. This is achieved by solving for \mathbf{u}_1 from Eq. (5) and substituting this expression for \mathbf{u}_1 into Eq. (6). The resulting equation is a quadratic equation for μ , and is

$$\begin{aligned} A^* \mu^2 - B^* \mu + C^* &= 0 \\ A^* &= \frac{\xi_{\perp} \cdot \xi_{\perp} \delta t^2}{8B_{1/2}} \\ B^* &= 1 + \frac{\delta t \xi_{\perp} \cdot (\hat{\mathbf{u}}_{\perp} - \mathbf{u}_{0\perp})}{2B_{1/2}} \\ C^* &= \frac{(\hat{\mathbf{u}}_{\perp} - \mathbf{u}_{0\perp}) \cdot (\hat{\mathbf{u}}_{\perp} - \mathbf{u}_{0\perp})}{2B_{1/2}} \end{aligned} \tag{7}$$

$$\left\{ \begin{matrix} \xi \\ \hat{\mathbf{u}} \end{matrix} \right\} = \frac{\mathbf{I} - \mathbf{I} \times \left(\frac{q\delta t}{2m} \mathbf{B}_{1/2} \right) + \left(\frac{q\delta t}{2m} \mathbf{B}_{1/2} \right) \left(\frac{q\delta t}{2m} \mathbf{B}_{1/2} \right)}{1 + \left(\frac{q\delta t}{2m} B_{1/2} \right)^2}$$

$$\left\{ \begin{matrix} \xi_{\perp} \\ \hat{\mathbf{u}}_{\perp} \\ \mathbf{u}_{0\perp} \end{matrix} \right\} = \left(\mathbf{I} - \frac{\mathbf{B}_{1/2} \mathbf{B}_{1/2}}{B_{1/2}^2} \right) \cdot \left\{ \begin{matrix} \xi \\ \hat{\mathbf{u}} \\ \mathbf{u}_0 \end{matrix} \right\},$$

where \mathbf{I} is the unit dyad. The quadratic equation for μ yields two roots. One can show that in order to obtain the correct asymptotic behavior for μ in the limits of small and large time steps, the following root for μ must be used:

$$\mu = \frac{1}{2A^*} (B^* - [(B^*)^2 - 4A^*C^*]^{1/2}). \tag{8}$$

Given \mathbf{x}_0 and \mathbf{u}_0 , one uses Eqs. (5) and (7)–(8) to calculate \mathbf{x}_1 and \mathbf{u}_1 . Note that one needs to have an iteration procedure, just as in Method II, to solve for \mathbf{x}_1 and \mathbf{u}_1 from Eqs. (5) and (7)–(8). For simplicity, we solve the equations approximately using a predictor–corrector iteration procedure.

3. RESULTS AND DISCUSSION

For the discussion at hand, the electric and magnetic fields are prescribed as

$$\begin{aligned} \mathbf{E} &= 0 \\ \mathbf{B} &= B_0 e^{x/L} \hat{\mathbf{z}}, \end{aligned} \tag{9}$$

where B_0 and L are constant. We consider only motion that is perpendicular to the magnetic field. At time $t = 0$, the particle position and perpendicular velocity are

$$\begin{aligned} \mathbf{r}_0 &= 0 \\ \mathbf{u}_0/c &= 0.1 \hat{\mathbf{y}}. \end{aligned}$$

Without any loss of generality, the particle’s charge-to-mass ratio (q/m) is chosen to be unity. Note that this case is constructed in such a way that the particle’s physical gyroradius is much smaller than L , the magnetic gradient scale length. Since the particle’s physical gyroradius is much smaller than the magnetic gradient scale length, one can use an analytical perturbation analysis to calculate the gyroradius and drift velocity:

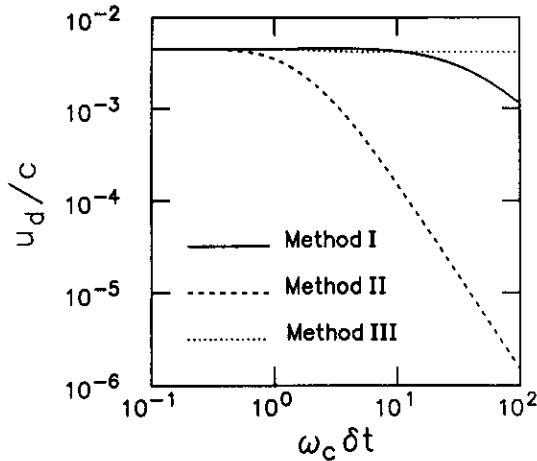


FIG. 1. A comparison of drift speed vs $\omega_c \delta t$ for Method I (leapfrog Boris algorithm), Method II (implicit Boris algorithm), and Method III (implicit Boris algorithm with $-\mu \nabla B$ correction).

$$\begin{aligned} \rho_0/L &\approx 0.09 \\ \mathbf{u}_d/c &\approx 0.0045\hat{y}. \end{aligned} \quad (10)$$

It should be noted here that for the magnetic field configuration given in Eqs. (9), the only drift motion possible is the gradient- B drift. The particle trajectory has also been calculated by integrating numerically the particle equations of motion using Methods I–III, and the results are shown in Figs. 1–2.

Figure 1 plots of the y -component of the particle's drift velocity as a function of $\omega_c \delta t$, indicates that for small time steps ($\omega_c \delta t < 1$), all three methods are in approximate agreement with the analytical value of the drift speed given by Eqs. (10). Method I (leapfrog Boris algorithm) continues to yield drift speeds comparable to the correct drift speed (given in Eqs. (10)) up to $\omega_c \delta t$ of 10. For larger values of the time step, the drift speed is lower than the correct value. Method II (implicit Boris algorithm) yields drift speeds considerably lower than the correct value for $\omega_c \delta t > 1$. Method III (implicit Boris algorithm with $-\mu \nabla B$ correction) yields drift speeds comparable to the correct drift speed for very large time steps, e.g., even at $\omega_c \delta t = 100$. In fact, one can easily show that as $\omega_c \delta t \rightarrow \infty$, while the drift speeds obtained from both Method I and Method II will tend to 0, the drift speed obtained from Method III will tend to a constant value comparable to the correct value given in Eqs. (10). In all three methods, the drift speeds in the x and z directions are zero, consistent with Eqs. (10).

Figure 2 plots of the numerical gyroradius versus $\omega_c \delta t$, indicates that for small time steps ($\omega_c \delta t < 1$) all three methods yield a value for the gyroradius that agrees with the correct gyroradius given in Eqs. (10). For large time steps ($\omega_c \delta t > 1$), Method I yields a gyroradius which increases with $\omega_c \delta t$. One can see why by taking the limit of Eq. (3) as δt becomes large.

In that limit, the average velocity perpendicular to the magnetic field is given by

$$\frac{\mathbf{u}_{\perp 1} + \mathbf{u}_{\perp 0}}{2} \sim O(1/\delta t). \quad (11)$$

Thus, with Method I,

$$\mathbf{u}_{\perp 1} \approx -\mathbf{u}_{\perp 0} + O(1/\delta t) \quad (12)$$

and for large δt , Eq. (2) gives

$$\mathbf{x}_{13/2} - \mathbf{x}_{11/2} \approx -\mathbf{u}_{\perp 0} \delta t. \quad (13)$$

From the definition of the gyroradius, $\rho_0 = |u_{\perp 0}|/\omega_c$, one finds the numerical gyroradius to be for large δt ,

$$\rho_c \approx \rho_0(\omega_c \delta t).$$

However, Method II and Method III continue to yield correct values for the gyroradius. For these methods, the displacement perpendicular to the magnetic field for large δt is given by

$$\lim_{\delta t \rightarrow \infty} |\mathbf{x}_{11} - \mathbf{x}_{10}| = 2|\mathbf{u}_{\perp 0}| \left| \frac{q\mathbf{B}}{m} \right| \quad (14)$$

which is the correct value.

Evidently, as the time step increases, $\omega_c \delta t > 1$, the increase in gyroradius with Method I compensates for numerical errors in the particle drift motion, resulting in approximately correct drift speeds until the gyroradius becomes comparable to the magnetic gradient scale length; i.e., the particle no longer sees a uniform magnetic field as it samples the orbit. With Method

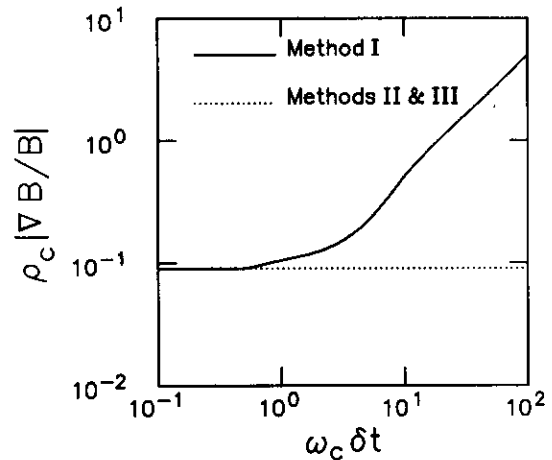


FIG. 2. A comparison of numerical gyroradius vs $\omega_c \delta t$ for Method I (leapfrog Boris algorithm), Method II (implicit Boris algorithm), and Method III (implicit Boris algorithm with $-\mu \nabla B$ correction).

I, the gyroradius will exceed the magnetic field gradient scale length unless

$$\omega_c \delta t < \frac{\rho_0}{B/|\nabla B|}. \quad (15)$$

Thus, in problems with nonuniform gradients in the magnetic field, Eq. (15) must be satisfied at every point for every particle. For the case presented in Figs. 1–2, Method I yields incorrect drift speeds for $\omega_c \delta t > 10$ because the numerical gyroradius exceeds the magnetic gradient scale length.

4. SUMMARY AND CONCLUSIONS

Our conclusion is that if the magnetic gradient scale length is spatially varying, the drift speeds obtained from Method I are not reliable for $\omega_c \delta t > 1$ unless Eq. (15) is satisfied. For large time steps ($\omega_c \delta t > 1$), Method II yields a gyroradius which is independent of the time step. As a result, numerical errors in the particle drift motion are not compensated (as is the case with Method I), and the drift speeds obtained are considerably less than the correct value. Our conclusion is that drift speeds obtained from Method II are not reliable for $\omega_c \delta t > 1$. For large time steps ($\omega_c \delta t > 1$), Method III, like Method II, yields a gyroradius which is independent of the time step. Numerical errors in the particle drift motion are compensated by adding an explicit $-\mu \nabla B$ correction. As a result, Method III yields the correct gyroradius and the correct drift speeds for arbitrarily large time steps. It is worthwhile to note that the magnetic moment μ defined in Eq. (6) is actually a function of $\omega_c \delta t$. For $\omega_c \delta t \ll 1$, $\mu \propto (\omega_c \delta t)^2$ and the contribu-

tion from $-\mu \nabla B$ is negligible. For $\omega_c \delta t \gg 1$, μ is independent of $\omega_c \delta t$ and takes on the correct value for the particle magnetic moment. As a result, Method III yields the correct drift speeds for arbitrarily large time steps.

Particle motion in magnetic fields with spatially varying gradients and with non-zero electric fields have been studied using Method III (results not shown). The results indicate that Method III yields approximately correct gyroradii and drift speeds for arbitrarily large time steps. Particle motion in magnetic mirrors was considered earlier for Method III [3].

ACKNOWLEDGMENT

This work was performed under the auspices of the U.S. Department of Energy.

REFERENCES

1. J. P. Boris "Relativistic Plasma Simulation—Optimization of a Hybrid Code," in *Proceedings, Fourth Conference on Numerical Simulation of Plasmas, Washington DC, November 1970*, pp. 3–67.
2. S. E. Parker and C. K. Birdsall, *J. Comput. Phys.* **97**, 91 (1991).
3. J. U. Brackbill and D. W. Forslund, in *Multiple Time Scales, Computational Techniques*, edited by J. U. Brackbill and B. I. Cohen (Academic Press, New York, 1985).
4. J. U. Brackbill and D. W. Forslund, *J. Comput. Phys.* **46**, 271 (1982).

Received February 4, 1994

H. X. VU
J. U. BRACKBILL

Applied Theoretical Physics
Los Alamos National Laboratory
Los Alamos, New Mexico 87545